HHS Public Access

Author manuscript

Chemosphere. Author manuscript; available in PMC 2016 March 06.

Published in final edited form as:

Chemosphere. 2016 February ; 144: 1106–1115. doi:10.1016/j.chemosphere.2015.09.045.

Enhanced and Stabilized Arsenic Retention in Microcosms through the Microbial Oxidation of Ferrous Iron by Nitrate

JING SUN[1,2], **STEVEN N. CHILLRUD**[2], **BRIAN J. MAILLOUX**[3], **MARTIN STUTE**[2,3], **RAJESH SINGH**[4], **HAILIANG DONG**[4], **CHRISTOPHER J. LEPRE**[2], and **BENJAMIN C. BOSTICK**[*,2]

[1]Department of Earth and Environmental Sciences, Columbia University, Mail Code 5505, New York, NY 10027

[2]Lamont-Doherty Earth Observatory, PO Box 1000, 61 Route 9W, Palisades, NY 10964

[3]Department of Environmental Sciences, Barnard College, 3009 Broadway, New York, NY 10027

[4]Department of Geology and Environmental Earth Science, Miami University, Oxford, OH 45056

Abstract

Magnetite strongly retains As, and is relatively stable under Fe(III)-reducing conditions common in aquifers that release As. Here, laboratory microcosm experiments were conducted to investigate a potential As remediation method involving magnetite formation, using groundwater and sediments from the Vineland Superfund site. The microcosms were amended with various combinations of nitrate, $Fe(II)_{(aq)}$(as ferrous sulfate) and lactate, and were incubated for more than 5 weeks. In the microcosms enriched with 10 mM nitrate and 5 mM $Fe(II)_{(aq)}$, black magnetic particles were produced, and As removal from solution was observed even under sustained Fe(III) reduction stimulated by the addition of 10 mM lactate. The enhanced As retention was mainly attributed to co-precipitation within magnetite and adsorption on a mixture of magnetite and ferrihydrite. Sequential chemical extraction, X-ray absorption spectroscopy and magnetic susceptibility measurements showed that these minerals formed at pH 6 – 7 following nitrate-Fe(II) addition, and As-bearing magnetite was stable under reducing conditions. Scanning electron microscopy and X-ray diffraction indicated that nano-particulate magnetite was produced as coatings on fine sediments, and no aging effect was detected on morphology over the course of incubation. These results suggest that a magnetite based strategy may be a long-term remedial option for As-contaminated aquifers.

GRAPHICAL ABSTRACT

[*]Corresponding author: phone: (845) 365-8659; fax: (845) 365-8155; bostick@ldeo.columbia.edu.

SUPPLEMENTARY MATERIAL

Tables S1 – S3 and Figures S1 – S7. The supplementary tables and figures contain information from previous publications regarding magnetite formation, Fe Eh-pH diagram, mass balance calculations, reference and sample Fe EXAFS spectra, detailed linear combination fitting results and quality of the fits, various XRD patterns, SEM images, and etc.

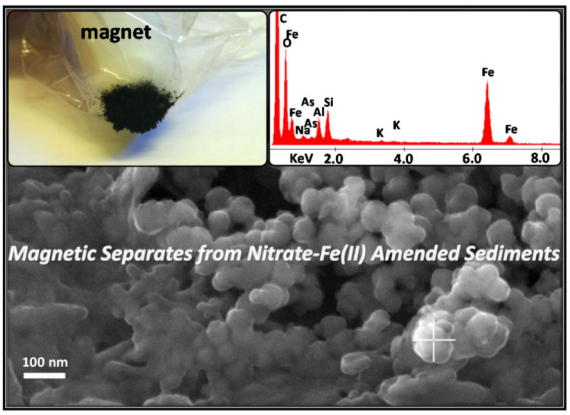

Keywords

Magnetite; Iron minerals; Arsenic concentration; Redox transformation; Microcosm experiment; Immobilization

1. INTRODUCTION

Arsenic is the 2nd most common contaminant of concern at the U.S. Superfund sites, with nearly 50% of sites having groundwater As related problems (ATSDR, 2013). Mitigating groundwater As contamination is urgently required, however, has proven difficult. Encapsulation technology, common in soil remediation, is typically impractical for diffuse contaminants. Pump-and-treat (P&T), which can control groundwater migration, is commonly used for groundwater remediation (EPA, 2003). This method is hampered for As because of slow and inefficient desorption from aquifer sediments (Wovkulich et al., 2012; Wovkulich et al., 2014). One attractive option for remediating groundwater As is *in situ* immobilization, which stimulates mineral formation within the aquifer to adsorb and/or precipitate As.

Iron minerals are commonly used as As sorbents (Benner et al., 2002; Dixit and Hering, 2003; Kneebone et al., 2002; Pedersen et al., 2006). The limited stability of Fe minerals under reducing conditions, however, represents a major challenge to the development of As *in situ* immobilization in aquifers. Reducing conditions common in aquifers can lead to reductive dissolution of many common Fe(III) (oxyhydr)oxide minerals, remobilizing the associated As (Benner et al., 2002). Arsenic can also adsorb on or co-precipitate within Fe(II) sulfide minerals (O'Day et al., 2004; Saalfield and Bostick, 2009). Sulfide-based As immobilization strategies can be effective under some conditions (Keimowitz et al., 2007; O'Day et al., 2004; Onstott et al., 2011), but these methods often are limited by sulfide mineral oxidation, and can be solubilized as thiolated As complexes in sulfidic solutions (Wilkin et al., 2003).

Magnetite, Fe_3O_4, is a mixed-valence Fe oxide containing both tetrahedral and octahedral Fe(III) (Coker et al., 2006; Schwertmann and Cornell, 2008). Unlike many Fe minerals, magnetite is stable in a wide range of conditions including Fe(III)-reducing environments

where As is typically mobilized and bioavailable (An Fe Eh-pH diagram is provided in the supplementary material (SM) Figure S1, also showing *in situ* redox conditions at selected Superfund sites) (deLemos et al., 2006; He et al., 2010; Keimowitz et al., 2005; Lipfert et al., 2006; Wovkulich et al., 2014), although biogenic and abiogenic magnetite may have different stability towards microbial Fe(III) reduction (Muehe et al., 2013b; Piepenbrock et al., 2011). Magnetite can scavenge both As(V) and As(III) from solutions through surface adsorption (Chowdhury et al., 2011; Gimenez et al., 2007; Pedersen et al., 2006; Wang et al., 2008; Yean et al., 2005). It is also capable of co-precipitating tetrahedral As(V) as well as a number of cations (e.g., Al^{3+}, Ti^{4+}, Cr^{3+}, Co^{2+}, Ni^{2+}, Cu^{2+}, Zn^{2+} and Cd^{2+}) into its crystal structure (Coker et al., 2006; Cooper et al., 2000; Jang et al., 2003; Muehe et al., 2013a; Saalfield and Bostick, 2009; Schwertmann and Cornell, 2008). So far, the potential of *in situ* immobilization of contaminants on magnetite has seldom been applied to groundwater remediation efforts. This is in part because magnetite is typically synthesized through reductive pathways of Fe(III) oxyhydroxides at pH >7.5 (SM Table S1), while aquifer pHs at As-contaminated sites are commonly circumneutral to acidic, i.e., conditions under which magnetite production through this pathway is inhibited (Ayala-Luis et al., 2008; Hansel et al., 2005; Jang et al., 2003; Jolivet et al., 2002; Schwertmann and Cornell, 2008; Tronc et al., 1992). Magnetite formation can also be stimulated by Fe(II)-oxidizing bacteria (Chaudhuri et al., 2001; Dippon et al., 2012), and dissolved As can be sequestered through such microbial oxidation (Hohmann et al., 2011; Hohmann et al., 2010; Senn and Hemond, 2002). Given the stability of magnetite under a relatively broad range of aquifer redox conditions, if reliably produced, it could not only achieve but maintain low groundwater As concentrations because magnetite is thermodynamically stable under aquifer conditions.

The objectives of the present study are to stimulate magnetite formation in amended microcosms containing natural aquifer sediments and groundwater, and to evaluate the effect on immobilizing As. The evolution of solution composition and sediment mineralogical transformations in microcosms were concurrently traced using several techniques. In all, our data suggest that magnetite formation can be achieved by the microbial oxidation of Fe(II) by nitrate, even under mildly acidic pH conditions, and that the combination of magnetite and other Fe oxides effectively sequesters dissolved As even under sustained Fe(III) reduction.

2. MATERIALS AND METHODS

2.1. Site Information and Sample Collection

This study uses aquifer sediments and groundwater from the Vineland Chemical Company Superfund site (Cumberland County, New Jersey). Descriptions of the Vineland site have been previously reported (Wovkulich et al., 2012; Wovkulich et al., 2014). Arsenic contamination here resulted from improper storage of As-containing herbicides and salts between 1949 and 1994. Before mitigation efforts, the Vineland aquifer sediments were contaminated with typical As concentrations of 20 to 250 mg kg^{-1}, and site groundwater As concentrations exceeded WHO drinking water standard (10 μg L^{-1} As) by up to three orders of magnitude. A large P&T system, as well as several other strategies, is involved in the

current mitigation activities at Vineland. The sediments used in this study were derived from a pit freshly dug down below the water table with a backhoe in an area that is weakly acidic (pH ~ 6), composed of orange-colored sandy grains. Immediately after retrieval, the sediments were homogenized and sealed in new metal cans. The groundwater used in this study was from a P&T well (RW 02) adjacent to the sediment collection location. The well was sufficiently flushed before collecting and sealing groundwater in plastic cubitainers (no filtering or poisoning of the groundwater). Aquifer sediments and groundwater were kept in the dark at 4 °C once collected and brought back to laboratory for experiments. The major element composition of this groundwater was stable, and although Fe precipitated from it, As concentration was similar to aquifer levels (Wovkulich et al., 2014).

2.2. Microcosm Setup: First Set of Microcosms

A series of microcosms (Table 1) were performed by mixing 26.5 g homogenized wet sediments (24.5 g in dry weight) with 490 mL groundwater, in 500 mL high-density polyethylene bottles. After mixing, sediments and groundwater were pre-equilibrated for 24 hours in sealed bottles. The microcosms were then treated on Day 0 in duplicate as following: (i) control (amendment-free), (ii) nitrate-only treatment (10 mM $NaNO_3$) and (iii) nitrate-Fe(II) treatment (10 mM $NaNO_3$ & 5 mM $FeSO_4$). Nitrate was chosen as the oxidant rather than oxygen because it is soluble and reacts slowly with ferrous Fe. The slow oxidation should limit mineral precipitation in field trials, thus preventing clogging in injection wells. Ferrous sulfate was chosen as the source of ferrous Fe because it is stable and readily available. For nitrate-Fe(II) treatment, since ferrous Fe hydrolyzes, particularly when oxidized, producing H^+, NaOH was added 24 hours after nitrate-Fe(II) addition to neutralize the ferrous Fe. To test the stability of the amended microcosms, 10 mM Na-lactate was added as a model organic carbon source to stimulate microbial activity and reducing conditions. Lactate was applied in nitrate-only and nitrate-Fe(II) treatments on Day 10.0 when solution compositions stabilized, which made them two-stage incubations with the beginning to Day 10.0 as nitrate-treated “oxidative” stage and Day 10.0 to the end as lactate-treated “reductive” stage. These microcosms were incubated simultaneously and semi-anaerobically in sealed bottles (oxygen was not excluded from headspace) at room temperature. The presence of some oxygen is relevant and necessary for the setup of microcosms with the Vineland sediments, since the sediments are somewhat oxic. The duration of this experiment was 38.0 days, during which the bottles were opened for subsampling approximately twice per week with < 2 minutes each time. During subsampling, microcosms were monitored for pH and Eh, and aliquots (i.e., sediment-groundwater mixture) were removed and filtered to 0.2 μm. The solutions were acidified and analyzed by inductively coupled plasma mass spectrometry (ICP-MS). The sediments contained on filter membranes were immediately coated in glycerol to prevent exposure to oxygen and sealed in microcentrifuge tubes in the dark at −20 °C for X-ray absorption spectroscopy (XAS) analysis.

2.3. Analytical Techniques

Solution samples from the microcosms were analyzed by Axiom Single Collector ICP-MS (Thermo Elemental) or Element XR ICP-MS (Thermo Fisher Scientific) for dissolved elemental concentrations. Germanium (Ge) was added as an internal response standard and

used for monitoring instrument drift. For As, resolving power of the instrument was set at around 10,000 to resolve the ^{75}As peak from Ar-Cl interference. Each sample was run three times and averaged. Quantification was based on comparison to a six-point standard curve for a multi-element standard. Accuracy was verified against known quality controls NIST 1640A and NIST 1643.

Initial Vineland aquifer sediments, and amended sediments on Day 12.5 and Day 38.0 from above microcosms, were analyzed for As X-ray absorption near edge structure (XANES) and Fe extended X-ray absorption fine structure (EXAFS) spectra. The analysis was carried out at the Stanford Synchrotron Radiation Laboratory (SSRL) on beamline 4-1. The beamline was configured with a Si(220) monochromator and a phi angle of 90 degrees. Soller slits were installed to minimize the effects of scattered primary radiation. The beam was detuned as needed to reject higher-order harmonic frequencies and prevent detector saturation. Sample fluorescence was measured in combination with 6 μx Mn filter for Fe and 6 μx Ge filter for As data, respectively, with a 13-element Ge detector. Arsenic XANES and Fe EXAFS spectra were processed in SIXpack software (Webb, 2005) using standard procedures (Saalfield and Bostick, 2009; Sun et al.; Wovkulich et al., 2014). Na-arsenate, Na-arsenite and orpiment (As_2S_3) were chosen as As references. Ferrihydrite, goethite, hematite, magnetite, siderite, mackinawite and Fe(III)-rich illite, were chosen as Fe references, consistent with an earlier (micro-XANES) study on Vineland aquifer (Wovkulich et al., 2014). Least-squares linear combination fitting (LCF) was used to quantify the percentage of each reference, which was then converted to the final amount by multiplying by bulk elemental concentration when needed. Quantitation based on standard-addition methods has shown that the detection limits of Fe EXAFS-LCF are adequate to quantify magnetite and ferrihydrite in such microcosms (Sun et al.).

2.4. Second Set of Microcosms and Analytical Techniques

To examine magnetite formation and its effect on As partitioning in more detail, a 2nd set of two nitrate-Fe(II) microcosms (Table 1) were performed identically to the 1st set (using stored groundwater and sediments, no new materials were collected from the Vineland site). One of the microcosms was incubated for 12.5 days and the other for 39.5 days. Again, lactate was applied in the microcosms on Day 10.0, microcosms were monitored for pH and Eh, and aliquots were subsampled and filtered to 0.2 μm. Each solution sample was analyzed for dissolved elemental concentrations by ICP-MS, and for dissolved organic carbon (DOC) by high-temperature catalytic oxidation method on a Shimadzu total organic carbon VCSN analyzer. Each sediment sample contained on filter membrane and coated with glycerol in a microcentrifuge tube, was measured for magnetic susceptibility with a Bartington MS2B instrument following collection. It was then dried after being washed by water, and dry mass of the sediments was obtained for susceptibility calculation. Aliquots were also subsampled and freeze dried on Day 4.5, Day 12.5 and Day 39.5. The freeze-dried sediments were ground to powder using an agate mortar-and-pestle set, and X-ray diffraction (XRD) patterns over 2-Theta range of 4° to 80° were collected using a PANalytical X'pert3 Powder diffractometer with Cu K-alpha radiation (λ = 1.5406 Å). Additionally, the remaining sediments after the last set of subsamples in each microcosm were freeze-dried, and magnetic particles were separated by a magnet. A subsample of the magnetic separates was

mounted over the scanning electron microscopy (SEM) sample stubs using flat sticky tabs and coated with carbon using Denton Vacuum Evaporator DV-502A. A Zeiss Supra 35 VP SEM with Genesis 2000 X-ray energy dispersive spectroscopy (EDS) was then employed for morphological and compositional analyses. The rest of the magnetic separates were diluted 50 wt% with boron nitride (BN), ground, and also analyzed by XRD.

Immediately after XRD analysis, the powders from the sediments and magnetic separate samples were subjected to sequential chemical extraction (Table 2) (Keon et al., 2001; Poulton and Canfield, 2005). Sediment samples were directly used, whereas the magnetic separates-BN mixtures were further diluted 80 wt% with pure quartz. Extractions were conducted with a dry mass size of 150 mg and an extractant volume of 10 mL, at room temperature in constantly agitated polyethylene centrifuge tubes. Extractants were prepared freshly, by dissolving chemicals in oxygen-free Milli-Q water (purged with N_2(g)). Extractions were performed in sealed tubes following purging with N_2(g). At the end of each extraction, suspensions were centrifuged. The supernatants were then filtered to 0.2 μm and analyzed by ICP-MS, and solids were treated with the next extractant. After extraction, elemental concentrations in residues were determined following microwave-assisted acid-digestion (EPA, 1995). To verify the experimental extraction/digestion procedure, As(V)-adsorbed magnetite and an As(V)-adsorbed ferrihydrite-goethite-magnetite mixtures were also prepared, diluted with BN and quartz, and simultaneously extracted/digested and analyzed. (More details on mineral synthesizing and sample processing are in SM Figure S2.)

3. RESULTS AND DISCUSSION

3.1. Iron Mineralogy and Arsenic Solubility in Different Microcosms

Based on XAS analyses (Figure 1 and 2), initial Vineland aquifer sediments used in this study contained mostly Fe(III) (97% ± 14% of total Fe) and As(V) (98% ± 1% of total As), and did not contain magnetite. Poorly-ordered ferrihydrite dominated the initial sediment Fe, which is an effective As adsorbent but susceptible to reductive transformations and often linked to the release of adsorbed As into solution under reducing conditions (Pedersen et al., 2006; Raven et al., 1998). Sediment As remained as As(V) in the microcosms over the course of incubation. Sediment Fe mineralogy and solution composition (Figure 3), however, changed considerably and varied widely between microcosm treatment types.

3.1.1. Controls and Nitrate-only Microcosms—In the controls without treatment, dissolved As concentrations increased slightly and gradually to a maximum of 815 μg L^{-1} (Figure 3A), due to sediment-solution equilibrium and probably driven by microbially mediated reactions with pre-existing organic carbon. Nitrate is known to strongly influence Fe and accordingly As, and also meditates As(III) oxidation to As(V) (Gibney and Nusslein, 2007; Hohmann et al., 2011; Senn and Hemond, 2002). The addition of 10 mM nitrate to the microcosms, however, was ineffective at altering solution composition (Figure 3). Subsequent addition of exogenous organic carbon encouraged reductive transformation of Fe(III) oxyhydroxides, and led to accumulation of secondary Fe(II)-containing minerals, including magnetite, siderite and mackinawite (Figure 1). Correspondingly, a dramatic

increase in dissolved As concentration (peaked at about 2 mg L^{-1}) was observed. The release of sediment As into solution resulted partially from the depletion of surface sites. Moreover, lactate addition caused a shift in pH from acidic to pH about 7.8 (Figure 3C), which is above the optimal pH for As(V) adsorption on Fe oxides (Chowdhury et al., 2011; Dixit and Hering, 2003). Bicarbonate production from lactate oxidation in Ca-containing solutions could also enhance As(V) desorption from ferrihydrite and presumably some other minerals (Saalfield and Bostick, 2010).

3.1.2. Nitrate-Iron(II) Microcosms—The simultaneous addition of 10 mM nitrate and 5 mM $Fe(II)_{(aq)}$ to microcosms yielded drastically different results compared to the nitrate-only treatment. The nitrate-Fe(II) microcosms remained slightly acidic over the course of incubation (Figure 3C). These microcosms effectively decreased dissolved As concentration to 6 μg L^{-1} within 1.0 day, and kept it relatively low during not only the nitrate-treated oxidative but also the lactate-treated reductive stage of the incubation, with As concentration being 36 μg L^{-1} at the end of the incubation (Figure 3A). Induced by the addition of 5 mM ferrous Fe, dissolved Fe concentration was high in the beginning (Figure 3B). Primarily attributed to the oxidation of ferrous Fe by nitrate (and some dissolved oxygen) and subsequent mineral precipitation, dissolved Fe concentration then dropped to values below 0.5 mg L^{-1} at the end of the incubation. As indicated by Fe EXAFS (Figure 1), Fe mineralogy in these nitrate-Fe(II) microcosms changed considerably, with ferrihydrite and goethite being produced dominantly in combination with lesser quantity of magnetite. All three Fe mineral products can serve as scavengers of dissolved As (Dixit and Hering, 2003), however, have vastly different stability towards redox transformation. The quantity of Fe needed for effective removal was studied in a series of additional microcosms in which Fe concentrations were varied. At least 5 mM ferrous Fe addition was needed to effectively sequester As within the sediments and, more importantly, prevent the release of As into solution during the reductive stage (SM Figure S4).

3.1.3. Additional Nitrate-Iron(II) Microcosms – Magnetic Separates—Another two nitrate-Fe(II) microcosms, with the exact same amount of nitrate-Fe(II) addition, provided characterization using magnetic susceptibility, sequential chemical extraction, XRD and SEM-EDS. Prior to nitrate-Fe(II) addition, pH in these microcosms was half a pH unit higher than that in the 1st set. However, the pH difference was stable and the solution composition was otherwise reproducible (Figure 4A). Consistently, dissolved As concentration remained low, being 14 μg L^{-1} on Day 39.5. Magnetic susceptibility measurements increased from near zero to more than 3000 (unitless, CGS units) over the first 10 days and then stabilized (Figure 4B), consistent with Fe EXAFS results showing the formation of magnetite during the oxidation of Fe(II) by nitrate. This high magnetic susceptibility is indicative of magnetite because other Fe minerals have much lower susceptibilities, but susceptibility is difficult to convert to concentration due to sample heterogeneity and magnetic properties that vary with mineral size, morphology and composition (Maher, 1988; Porsch et al., 2010). Similar to the 1st set, amended sediments visibly contained black particles, which could be collected through magnetic separation once freeze dried. XRD confirmed the prevalence of magnetite and quartz in magnetic separates (Figure 5A and 5C) but was insensitive to trace phases, including magnetite, in unaltered

sediments (SM Figure S5). Iron sequential extractions can provide a means of (indirectly) determining Fe mineralogy in sediments and in magnetic separates (Figure 6) (Poulton and Canfield, 2005). Extractions on amended sediments indicated precipitation of a mineral assemblage of ferrihydrite, goethite and magnetite, which is similar to the 1st set but has a much higher fraction of magnetite probably owing to higher pH (Cooper et al., 2000; Jang et al., 2003). Extractions also indicated that about 45% (w/w) of the magnetic particles were Fe oxides (calculation is in SM Table S3), with the mineral composition generally being consistent with the composition derived from the characterization of amended sediments.

The magnetite, which was identified by Fe EXAFS, magnetic susceptibility, XRD, and extractions, can have a variety of morphologies that affect ion retention properties. XRD diffraction lines for magnetite exhibited line broadening typical of nanoparticles (Figure 5B and 5D). The full width at half maximum (FWHM) value of 0.39° and 0.42° of the largest magnetite diffraction line at 35.5° 2-Theta corresponds to a Scherrer domain size of 22 nm and 21 nm (Scherrer, 1918). Quartz, which is highly crystalline, had a FWHM of 0.07° on the diffractometer, which indicates that the magnetite width was not significantly affected by instrumental broadening. Thus the calculated Scherrer width is representative of the actual scattering domain size. This size agreed with high-magnification SEM images of these magnetic separates, which displayed about 30 nm cubic and botryoidal crystal habits and no sign of morphology change over the course of incubation (Figure 5C and 5E, additional SEM images are in SM Figure S6). SEM-EDS analysis also indicated the significant presence of Fe minerals which existed as coatings on the surface of quartz and other minerals.

3.2. Magnetite Formation Mechanism

The nitrate-Fe(II)-enriched microcosms produced considerable quantities of magnetite and other Fe oxides at neutral to acidic pH, i.e., conditions are not specifically favorable for magnetite formation (SM Table S1). There are two principal formation mechanisms for magnetite (Hansel et al., 2005; Schwertmann and Cornell, 2008): (1) $Fe(II)_{(aq)}$-induced (re)crystallization of ferrihydrite or other Fe(III) minerals, and (2) $Fe(II)_{(aq)}$ and $Fe(III)_{(aq)}$ co-precipitation:

$$Fe^{2+} + 2Fe(OH)_3\,(s) \rightarrow Fe_3O_4\,(s) + 2H^+ + 2H_2O \quad (1)$$

$$Fe^{2+} + 2Fe^{3+} + 4H_2O \rightarrow Fe_3O_4\,(s) + 8H^+ \quad (2)$$

Under reducing conditions, the reductive transformation of Fe(III) minerals (Reaction 1) usually directs the generation of magnetite. In such systems, small quantities of $Fe(II)_{(aq)}$ that are released through Fe(III) reduction trigger magnetite nucleation (Benner et al., 2002). The magnetite produced after lactate addition in the nitrate-only microcosms, which stimulated Fe(III)-reducing bacteria and generated $Fe(II)_{(aq)}$, should be mainly governed by this reductive pathway. However, in the nitrate-Fe(II) microcosms, according to DOC measurements (Figure 4A), Fe EXAFS, magnetic susceptibility, and extraction, (1) the majority of magnetite formation preceded the large consumption of organic carbon (Figure 4B and Figure 6), when microcosms were somewhat oxidized; and (2) other than magnetite,

goethite was the dominant mineral product following consumption of organic carbon (Figure 1 and Figure 6), when reductive transformation of ferrihydrite was active. We hypothesize that magnetite formation occurs through a microbial nitrate-involved oxidative pathway (Reaction 3) under the experimental conditions:

$$15Fe^{2+} + 2NO_3^- + 14H_2O \rightarrow 5Fe_3O_4\,(s) + N_2\,(g) + 28H^+ \quad (3)$$

The overall pathway involves the partial oxidation of excessive $Fe(II)_{(aq)}$ by nitrate and then the $Fe(II)_{(aq)}$ and $Fe(III)_{(aq)}$ co-precipitation (Reaction 2). The Gibbs energy of Reaction 3 illustrates the favorability of the oxidative pathway (ΔG_{rxn}, SM Figure S7). At pH 6, ΔG_{rxn} is −869.3 kJ mol^{-1} when ferrous Fe and nitrate were introduced (5 mM $Fe(II)_{(aq)}$ and 10 mM nitrate) and is −612.9 kJ mol^{-1} even when relevant reaction constituents were largely consumed (5 μM $Fe(II)_{(aq)}$ and 9 mM nitrate). Direct chemical oxidation of Fe(II) by nitrate is very slow, and probably not significant in these microcosms. Reaction 3, therefore, is a microbial process. Because these microcosms contained excess nitrate, denitrification likely occurred in parallel to Reaction 3. Additional magnetite could be formed by reaction with nitrite, produced during this denitrification, and $Fe(II)_{(aq)}$ (Melton et al., 2014):

$$9Fe^{2+} + 2NO_2^- + 8H_2O \rightarrow 3Fe_3O_4\,(s) + N_2\,(g) + 16H^+ \quad (4)$$

Dissolved oxygen levels were low in such microcosms, but residual oxygen might have been responsible for the oxidation of small quantities of $Fe(II)_{(aq)}$. However, the rate of oxidation appeared to be relatively slow (with 12 ~ 13 mg L^{-1} of dissolved Fe still present after 10 days of reaction, Figure 3B), which is largely consistent with typical rates of nitrate-dependent microbial oxidation (Straub et al., 1996). Many chemoautotrophs that can mediate the oxidation of ferrous Fe by nitrate are encountered in groundwater, freshwater, and marine environments (Hohmann et al., 2011; Jiao et al., 2005; Pantke et al., 2012; Senn and Hemond, 2002), and several appear to facilitate magnetite formation (Chaudhuri et al., 2001; Dippon et al., 2012; Miot et al., 2014; Zhao et al., 2013). Similar bacteria are likely to be present in the Vineland aquifer and experiments to characterize these species in these and other sediments are an ongoing effort. Magnetite, regardless of how it is formed, is relatively stable over a wide range of pH and redox conditions, and thus is less susceptible to reductive dissolution, which affects the suitability of other common Fe minerals (SM Figure S1) as As scavengers.

3.3. Arsenic Retention by Precipitated Iron Mineral Assemblage

In the nitrate-Fe(II) microcosms, aqueous As was incorporated into the solid phase upon Fe mineral precipitation. Sequential extractions of sediments and magnetic separates were used to estimate which of these Fe minerals were the most important for enhanced As retention. The extraction data indicated that the magnetic separates, which were enriched in magnetite, were also highly enriched with As (Figure 7). These magnetic separates contained 1434 mg kg^{-1} As at the end of incubation, 12x the concentration found in the Vineland sediments prior to any treatment. (Relevant mass balance calculations are in SM Table S3).

At least a portion of the As in the nitrate-Fe(II) microcosms is also bound to ferrihydrite, which has a high adsorption capacity and fast adsorption kinetics for As(V) (Dixit and

Hering, 2003; Raven et al., 1998). However, despite the fact that ferrihydrite is susceptible to reductive dissolution, As was not released from the nitrate-Fe(II) amended sediments even under the reductive stage of the incubation. This is in stark contrast to dramatic As release observed in the nitrate-only microcosms and in numerous reductive model systems that contain As-bearing ferrihydrite (Pedersen et al., 2006). The Fe(II)-catalyzed transformation of ferrihydrite to more stable phases could affect As partitioning. In these nitrate-Fe(II) microcosms, a part of the $Fe(II)_{(aq)}$ adsorbed on ferrihydrite and catalyzed mineral transformation to less reactive crystalline goethite (Figure 1 and Figure 6). Arsenic adsorption on goethite could have contributed to the stability of As retention, but this conversion also lowered surface area and thereby the amount of As adsorption (Gimenez et al., 2007).

We used a combination of sequential extractions and spectroscopy to show that a combination of adsorption to and co-precipitation within magnetite helped maintain low dissolved As concentrations during reduction. Of these, As incorporation into the crystal lattice of magnetite would be advantageous for remediation because magnetite (1) is thermodynamically stable under a wide range of pH and redox conditions (SM Figure 1) and (2) is kinetically stable, with As release only being possible in conjunction with slow mineral dissolution. Sequential extractions indicated that a quarter of the As in the nitrate-Fe(II) microcosms was bound within magnetite structure, and that a similar fraction of As was adsorbed to the magnetite surface (Figure 7). Coker et al. (2006) identified two distinct broad peaks at 11883 and 11895 eV in As XANES spectra of structural As(V) in magnetite. The As XANES spectra of nitrate-Fe(II) amended sediments is distinct from spectra of the other samples (Figure 2), although the diagnostic broad peaks are not obvious due to combined spectral contributions from several phases of solid As, presumably including As(V) within magnetite structure, and As(V) on the surfaces of ferrihydrite, goethite and magnetite. During the reductive stage, the fraction of As adsorbed to magnetite increased considerably, far beyond the levels of As associated with crystalline oxides such as goethite (Figure 7). The preference for magnetite is in part due to its nano-particulate size and associated with that high surface area (Figure 5). Even if Fe(III) reduction had further proceeded and completed reductive dissolution/transformation of both ferrihydrite and goethite, the amount of magnetite that prevailed in the nitrate-Fe(II) microcosms would have provided sufficient surface sites for all the associated As (Dixit and Hering, 2003; Gimenez et al., 2007).

4. IMPLICATIONS TO FUTURE REMEDIATION EFFORTS

This study represents an initial attempt to produce relatively stable As sequesters by simultaneous addition of ferrous Fe and nitrate, which can be achieved under neutral to mildly acidic pH conditions common in subsurface systems and appears to effectively immobilize As. Magnetite is one of the minerals produced by nitrate-Fe(II) addition. Since (1) magnetite could incorporate As into its structure during formation and could continue to sequester As through adsorption after formation, and (2) magnetite is less susceptible to redox changes under typical aquifer conditions, magnetite might serve as an advantageous host-mineral for As immobilization. This strategy was investigated using groundwater and sediments from the Vineland Superfund site, which contains mostly As(V), but could be

effective at many other sites with weakly reducing conditions. Arsenic(III) also adsorbs on magnetite, and if oxidized to As(V), could also be incorporated into magnetite (Amstaetter et al., 2009; Chowdhury et al., 2011; Dixit and Hering, 2003; Wang et al., 2008). The current nitrate-Fe(II) amendment also produced ferrihydrite which is vulnerable to reductive dissolution. To be a feasible remediation strategy for groundwater As contamination, the composition of the amendments probably need to be further refined such that less ferrihydrite is produced. One approach could be to decrease the rate of $Fe(III)_{(aq)}$ production so that there would be enough $Fe(II)_{(aq)}$ to be co-precipitated into magnetite (Jolivet et al., 1992). To achieve this, the optimal pH, Fe(II) and nitrate concentrations should be determined, and dissolved oxygen should be more strictly excluded. Since ferrihydrite might play a role in the efficiency of As removal, investigations are also required on whether less ferrihydrite production would affect the overall effectiveness of the strategy. Specialized bacterial strains could also be used to control particle size, or to enhance specific metabolic pathways following nitrate-Fe(II) addition. The presence of other solutes also could impact As retention on minerals, by competing for surface sites, or influencing mineral morphology and properties (Larese-Casanova et al., 2010; Porsch et al., 2010; Schwertmann and Cornell, 2008). Continued efforts are required, through both laboratory experiments and *in situ* trials, to establish and improve this remedial strategy. Reactive transport modeling of experimental data will also be useful to better understand the biogeochemical processes that affect treatment, and to evaluate the long-term potential of remedial action.

Supplementary Material

Refer to Web version on PubMed Central for supplementary material.

ACKNOWLEDGEMENTS

This study was funded by National Institute of Environmental Health Sciences (ES010349 and ES009089) and U.S. Department of Agriculture (2007-03128). Some of the analyses were carried out at SSRL, a national user facility operated by Stanford University for the U.S. Department of Energy. We are grateful to J. Ross, M. Fleisher, J. Mey, T. Ellis, Y. Zhong and A. Juhl for assistance with analyses at Columbia University, and to J. Rogers for technical support during XAS data collection. We would like to thank A. van Geen and P. Schlosser for helpful discussions, and B. Maher for comments on the magnetic measurements. We also would like to thank two anonymous reviewers for their insights. This is LDEO contribution number 7928.

REFERENCES

Amstaetter K, Borch T, Larese-Casanova P, Kappler A. Redox transformation of arsenic by Fe (II)-activated goethite (α-FeOOH). Environmental science & technology. 2009; 44(1):102–108. [PubMed: 20039739]

ATSDR. Summary data for 2013 priority list of hazardous substances. 2013. http://www.atsdr.cdc.gov/SPL/resources/ATSDR_2013_SPL_Detailed_Data_Table.pdf

Ayala-Luis KB, Koch CB, Hansen HCB. The Standard Gibbs Energy of Formation of Fe(II)Fe(III) Hydroxide Sulfate Green Rust. Clays and Clay Minerals. 2008; 56(6):633–644.

Benner SG, Hansel CM, Wielinga BW, Barber TM, Fendorf S. Reductive dissolution and biomineralization of iron hydroxide under dynamic flow conditions. Environmental Science & Technology. 2002; 36(8):1705–1711. [PubMed: 11993867]

Chaudhuri SK, Lack JG, Coates JD. Biogenic magnetite formation through anaerobic biooxidation of Fe(II). Applied and Environmental Microbiology. 2001; 67(6):2844–2848. [PubMed: 11375205]

Chowdhury SR, Yanful EK, Pratt AR. Arsenic removal from aqueous solutions by mixed magnetite-maghemite nanoparticles. Environmental Earth Sciences. 2011; 64(2):411–423.

Coker VS, et al. XAS and XMCD evidence for species-dependent partitioning of arsenic during microbial reduction of ferrihydrite to magnetite. Environmental Science & Technology. 2006; 40(24):7745–7750. [PubMed: 17256522]

Cooper DC, Picardal F, Rivera J, Talbot C. Zinc immobilization and magnetite formation via ferric oxide reduction by Shewanella putrefaciens 200. Environmental Science & Technology. 2000; 34(1):100–106.

deLemos JL, Bostick BC, Renshaw CE, Sturup S, Feng XH. Landfill-stimulated iron reduction and arsenic release at the Coakley Superfund Site (NH). Environmental Science & Technology. 2006; 40(1):67–73. [PubMed: 16433334]

Dippon U, Pantke C, Porsch K, Larese-Casanova P, Kappler A. Potential function of added minerals as nucleation sites and effect of humic substances on mineral formation by the nitrate-reducing Fe (II)-oxidizer Acidovorax sp. BoFeN1. Environmental Science & Technology. 2012; 46(12):6556–6565. [PubMed: 22642801]

Dixit S, Hering JG. Comparison of arsenic(V) and arsenic(III) sorption onto iron oxide minerals: Implications for arsenic mobility. Environmental Science & Technology. 2003; 37(18):4182–4189. [PubMed: 14524451]

EPA, U.S.. Method 3052: Microwave assisted acid digestion of siliceous and organically based matrices. Test Methods for Evaluating Solid Waste. 1995.

EPA, U.S.. Improving Nationwide Effectiveness of Pump-and-Treat Remedies Requires Sustained and Focused Action to Realize Benefits Report. EPA Office of Inspector General; 2003. Memorandum Report 2003-P-000006

Gibney BP, Nusslein K. Arsenic sequestration by nitrate respiring microbial communities in urban lake sediments. Chemosphere. 2007; 70(2):329–336. [PubMed: 17935754]

Gimenez J, Martinez M, de Pablo J, Rovira M, Duro L. Arsenic sorption onto natural hematite, magnetite, and goethite. Journal of Hazardous Materials. 2007; 141(3):575–580. [PubMed: 16978766]

Hansel CM, Benner SG, Fendorf S. Competing Fe(II)-induced mineralization pathways of ferrihydrite. Environmental Science & Technology. 2005; 39(18):7147–7153. [PubMed: 16201641]

He YT, et al. Geochemical processes controlling arsenic mobility in groundwater: A case study of arsenic mobilization and natural attenuation. Applied Geochemistry. 2010; 25(1):69–80.

Hohmann C, et al. Molecular-level modes of As binding to Fe(III) (oxyhydr)oxides precipitated by the anaerobic nitrate-reducing Fe(II)-oxidizing Acidovorax sp strain BoFeN1. Geochimica Et Cosmochimica Acta. 2011; 75(17):4699–4712.

Hohmann C, Winkler E, Morin G, Kappler A. Anaerobic Fe(II)-Oxidizing Bacteria Show As Resistance and Immobilize As during Fe(III) Mineral Precipitation. Environmental Science & Technology. 2010; 44(1):94–101. [PubMed: 20039738]

Jang JH, Dempsey BA, Catchen GL, Burgos WD. Effects of Zn(II), Cu(II), Mn(II), Fe(II), NO_3^-, or SO_4^{2-} at pH 6.5 and 8.5 on transformations of hydrous ferric oxide (HFO) as evidenced by Mossbauer spectroscopy. Colloids and Surfaces a-Physicochemical and Engineering Aspects. 2003; 221(1-3):55–68.

Jiao Y, Kappler A, Croal LR, Newman DK. Isolation and characterization of a genetically tractable photoautotrophic Fe (II)-oxidizing bacterium, Rhodopseudomonas palustris strain TIE-1. Applied and Environmental Microbiology. 2005; 71(8):4487–4496. [PubMed: 16085840]

Jolivet JP, Belleville P, Tronc E, Livage J. Influence of Fe(II) on the Formation of the Spinel Iron-Oxide in Alkaline-Medium. Clays and Clay Minerals. 1992; 40(5):531–539.

Jolivet JP, Tronc E, Chaneac C. Synthesis of iron oxide-based magnetic nanomaterials and composites. Comptes Rendus Chimie. 2002; 5(10):659–664.

Keimowitz AR, et al. Laboratory investigations of enhanced sulfate reduction as a groundwater arsenic remediation strategy. Environmental Science & Technology. 2007; 41(19):6718–6724. [PubMed: 17969686]

Keimowitz AR, et al. Naturally occurring arsenic: Mobilization at a landfill in Maine and implications for remediation. Applied Geochemistry. 2005; 20(11):1985–2002.

Keon NE, Swartz CH, Brabander DJ, Harvey CF, Hemond HF. Validation of an arsenic sequential extraction method for evaluating mobility in sediments. Environmental Science & Technology. 2001; 35(13):2778–2784. [PubMed: 11452609]

Kneebone PE, O'Day PA, Jones N, Hering JG. Deposition and fate of arsenic in iron- and arsenic-enriched reservoir sediments. Environmental Science & Technology. 2002; 36(3):381–386. [PubMed: 11871552]

Larese-Casanova P, Haderlein SB, Kappler A. Biomineralization of lepidocrocite and goethite by nitrate-reducing Fe(II)-oxidizing bacteria: Effect of pH, bicarbonate, phosphate, and humic acids. Geochimica Et Cosmochimica Acta. 2010; 74(13):3721–3734.

Lipfert G, Reeve AS, Sidle WC, Marvinney R. Geochemical patterns of arsenic-enriched ground water in fractured, crystalline bedrock, Northport, Maine, USA. Applied Geochemistry. 2006; 21(3): 528–545.

Maher BA. Magnetic-Properties of Some Synthetic Sub-Micron Magnetites. Geophysical Journal-Oxford. 1988; 94(1):83–96.

Melton ED, Swanner ED, Behrens S, Schmidt C, Kappler A. The interplay of microbially mediated and abiotic reactions in the biogeochemical Fe cycle. Nature Reviews Microbiology. 2014

Miot J, et al. Formation of single domain magnetite by green rust oxidation promoted by microbial anaerobic nitrate-dependent iron oxidation. Geochimica Et Cosmochimica Acta. 2014; 139:327–343.

Muehe EM, et al. Organic Carbon and Reducing Conditions Lead to Cadmium Immobilization by Secondary Fe Mineral Formation in a pH-Neutral Soil. Environmental Science & Technology. 2013a; 47(23):13430–13439. [PubMed: 24191747]

Muehe EM, Scheer L, Daus B, Kappler A. Fate of arsenic during microbial reduction of biogenic versus abiogenic As–Fe (III)–mineral coprecipitates. Environmental science & technology. 2013b; 47(15):8297–8307. [PubMed: 23806105]

O'Day PA, Vlassopoulos D, Root R, Rivera N. The influence of sulfur and iron on dissolved arsenic concentrations in the shallow subsurface under changing redox conditions. Proceedings of the National Academy of Sciences of the United States of America. 2004; 101(38):13703–13708. [PubMed: 15356340]

Onstott TC, Chan E, Polizzotto ML, Lanzon J, DeFlaun MF. Precipitation of arsenic under sulfate reducing conditions and subsequent leaching under aerobic conditions. Applied Geochemistry. 2011; 26(3):269–285.

Pantke C, et al. Green Rust Formation during Fe(II) Oxidation by the Nitrate-Reducing Acidovorax sp. Strain BoFeN1. Environmental Science & Technology. 2012; 46:1439–1446. [PubMed: 22201257]

Pedersen HD, Postma D, Jakobsen R. Release of arsenic associated with the reduction and transformation of iron oxides. Geochimica Et Cosmochimica Acta. 2006; 70(16):4116–4129.

Piepenbrock A, Dippon U, Porsch K, Appel E, Kappler A. Dependence of microbial magnetite formation on humic substance and ferrihydrite concentrations. Geochimica et Cosmochimica Acta. 2011; 75(22):6844–6858.

Porsch K, Dippon U, Rijal ML, Appel E, Kappler A. In-Situ Magnetic Susceptibility Measurements As a Tool to Follow Geomicrobiological Transformation of Fe Minerals. Environmental Science & Technology. 2010; 44(10):3846–3852. [PubMed: 20426439]

Poulton SW, Canfield DE. Development of a sequential extraction procedure for iron: implications for iron partitioning in continentally derived particulates. Chemical Geology. 2005; 214(3-4):209–221.

Raven KP, Jain A, Loeppert RH. Arsenite and arsenate adsorption on ferrihydrite: Kinetics, equilibrium, and adsorption envelopes. Environmental Science & Technology. 1998; 32(3):344–349.

Saalfield SL, Bostick BC. Changes in Iron, Sulfur, and Arsenic Speciation Associated with Bacterial Sulfate Reduction in Ferrihydrite-Rich Systems. Environmental Science & Technology. 2009; 43(23):8787–8793. [PubMed: 19943647]

Saalfield SL, Bostick BC. Synergistic effect of calcium and bicarbonate in enhancing arsenate release from ferrihydrite. Geochimica Et Cosmochimica Acta. 2010; 74(18):5171–5186.

Scherrer P. Bestimmung der Grösse und der inneren Struktur von Kolloidteilchen mittels Röntgenstrahlen. Nachrichten von der Gesellschaft der Wissenschaften zu Göttingen, mathematisch-physikalische Klasse. 1918; 1918:98–100.

Schwertmann, U.; Cornell, RM. Iron oxides in the laboratory. John Wiley & Sons; 2008.

Senn DB, Hemond HF. Nitrate controls on iron and arsenic in an urban lake. Science. 2002; 296(5577):2373–2376. [PubMed: 12089437]

Straub KL, Benz M, Schink B, Widdel F. Anaerobic, nitrate-dependent microbial oxidation of ferrous iron. Applied and Environmental Microbiology. 1996; 62(4):1458–1460. [PubMed: 16535298]

Sun J, Mailloux BJ, Chillrud SN, van Geen A, Bostick BC. Quantifying Ferrihydrite in Sediments by the Method of Standard-Additions Using EXAFS Spectroscopy. Environ. Sci. Technol. submitted.

Tronc E, Belleville P, Jolivet JP, Livage J. Transformation of Ferric Hydroxide into Spinel by Fe(II) Adsorption. Langmuir. 1992; 8(1):313–319.

Wang YH, et al. Arsenite sorption at the magnetite-water interface during aqueous precipitation of magnetite: EXAFS evidence for a new arsenite surface complex. Geochimica Et Cosmochimica Acta. 2008; 72(11):2573–2586.

Webb SM. SIXpack: a graphical user interface for XAS analysis using IFEFFIT. Physica Scripta. 2005; T115:1011–1014.

Wilkin RT, Wallschlager D, Ford RG. Speciation of arsenic in sulfidic waters. Geochem. Trans. 2003; 4(1):1–7.

Wovkulich K, et al. Use of microfocused X-ray techniques to investigate the mobilization of arsenic by oxalic acid. Geochimica Et Cosmochimica Acta. 2012; 91:254–270. [PubMed: 23175572]

Wovkulich K, et al. In Situ Oxalic Acid Injection to Accelerate Arsenic Remediation at a Superfund Site in New Jersey. Environmental Chemistry. 2014

Yean S, et al. Effect of magnetite particle size on adsorption and desorption of arsenite and arsenate. Journal of Materials Research. 2005; 20(12):3255–3264.

Zhao LD, et al. Biological oxidation of Fe(II) in reduced nontronite coupled with nitrate reduction by Pseudogulbenkiania sp Strain 2002. Geochimica Et Cosmochimica Acta. 2013; 119:231–247.

HIGHLIGHTS

- Magnetite is advantageous as the host-mineral for As immobilization.
- We conduct microcosms with sediment and groundwater from an As-contaminated site.
- We trace the evolution of water composition and sediment mineralogy concurrently.
- Addition of ferrous Fe and nitrate produces mineral assemblage including magnetite.
- The study represents an initial attempt to produce relatively stable As sequesters.

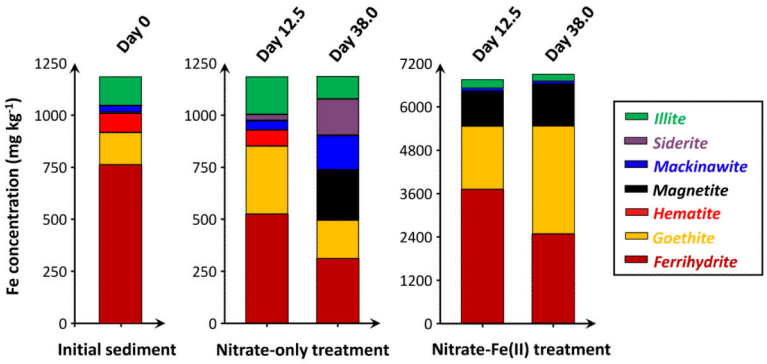

Figure 1.

Iron mineralogy in the sediments prior to any treatment (initial sediments) and in the sediments amended with different treatments, determined by Fe EXAFS-LCF (spectra and fits are in SM Figure S3 and Table S2). Concentrations are provided on a dry mass basis. Sediment samples from duplicate microcosms were combined before analysis.

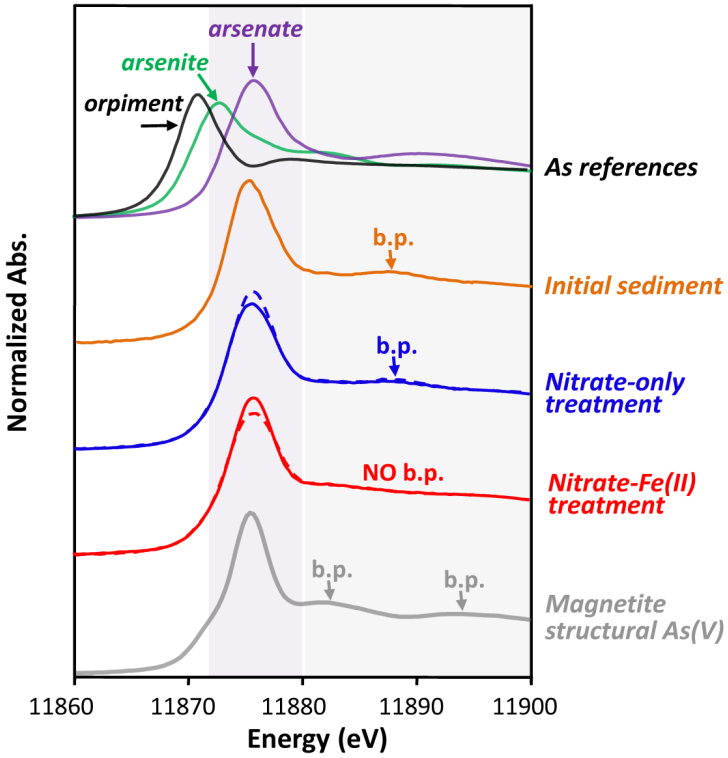

Figure 2.

Normalized As XANES spectra. The spectra are vertically offset for clarity. Sediment samples from duplicate microcosms were combined before analysis, dashed lines – Day 12.5, solid lines – Day 38.0. Reference spectra are included for comparison. Arsenic XANES of magnetite structural As(V) was obtained from Saalfield and Bostick (2009), showing broad peaks (b.p.) at 11883 eV and 11895 eV.

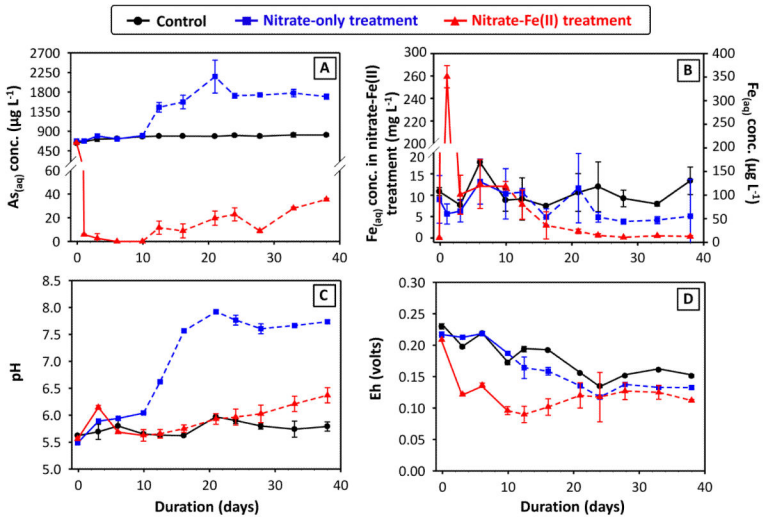

Figure 3.

Dissolved (A) As and (B) Fe concentrations, and (C) pH and (D) Eh, from the 1st set of microcosms as a function of time. The starting points (time = −0.05 ~ −0.04 day) are from the pre-equilibrated microcosms right before the addition of amendments (defined as time zero). The dashed lines, beginning at 10 days, indicate the portion of the microcosm experiment where lactate was present to stimulate reducing environment. Errors represent standard deviations between duplicate microcosms, some of which are smaller than the size of symbols used. For clarity, in subplot (B), dissolved Fe concentrations from nitrate-Fe(II) treatment were plotted on the primary y-axis, whereas those from the control and nitrate-only treatment were plotted on the secondary y-axis.

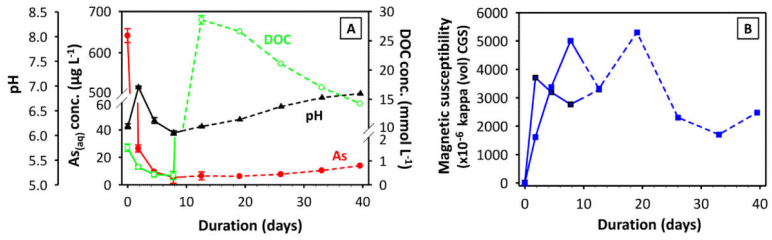

Figure 4.

(A) Dissolved As concentration, DOC centration, and pH from the 2nd set of nitrate-Fe(II) microcosms. The dashed lines indicate the time at which lactate was amended to stimulate a reducing environment. Errors were computed from duplicate microcosms, where available. (B) Magnetic susceptibility values for sediment, with two lines standing for two microcosms.

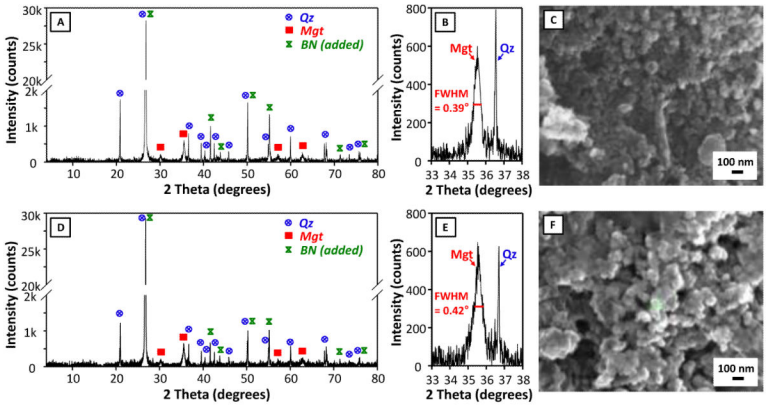

Figure 5.

XRD patterns of magnetic separates from the 2nd set of nitrate-Fe(II) microcosms with Cu K-alpha radiation (λ = 1.5406 Å), both full range and range focused on the magnetite 35.5° diffraction peak, and SEM images. (A)(B)(C) Showing magnetic separates from Day 12.5. (D)(E)(F) Showing magnetic separates from Day 39.5. Quartz – Qz, magnetite – Mgt, and boron nitrite – BN.

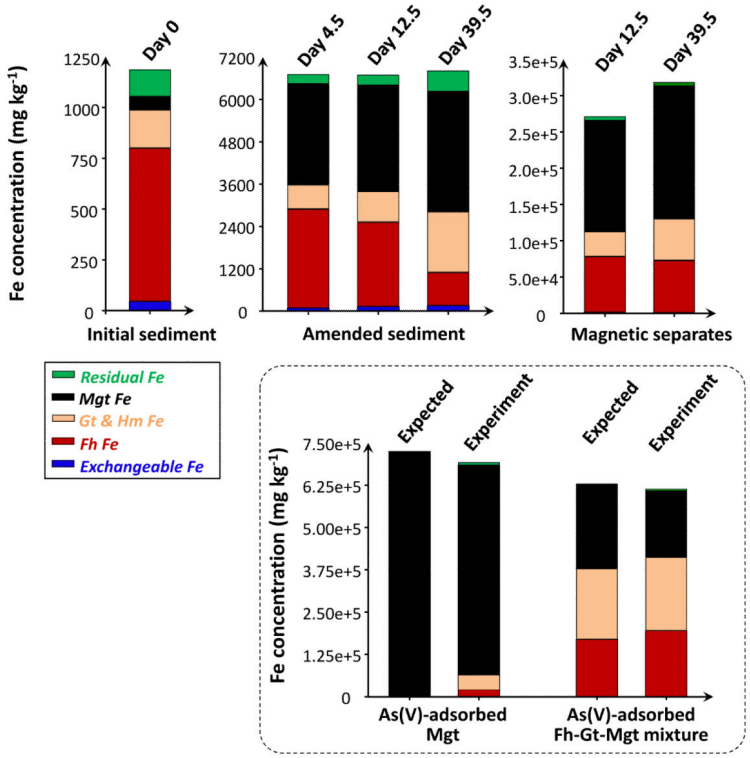

Figure 6.

Recoveries of Fe in the various extraction/digestion steps from (i) sediments prior to treatment (ii) amended sediments and magnetic separates from the 2nd set of nitrate-Fe(II) microcosms. The procedure was validated on As(V)-adsorbed magnetite and an As(V)-adsorbed Fe mineral mixture. Magnetite – Mgt, ferrihydrite – Fh, goethite – Gt, and hematite – Hm.

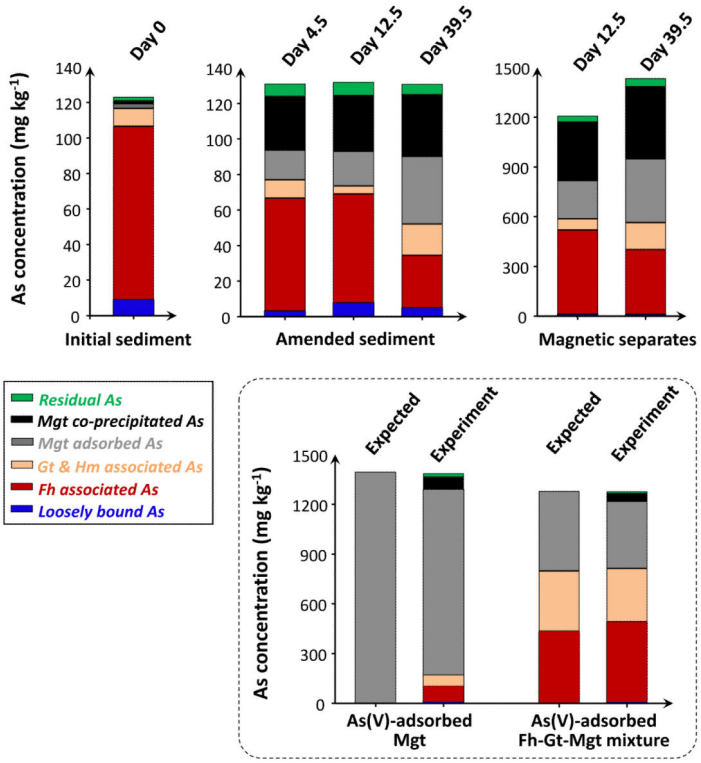

Figure 7.

Recoveries of As in the various extraction/digestion steps from (i) sediments prior to treatment (ii) amended sediments and magnetic separates from the 2nd set of nitrate-Fe(II) microcosms. The procedure was validated on As(V)-adsorbed magnetite and an As(V)-adsorbed Fe mineral mixture. Magnetite – Mgt, ferrihydrite – Fh, goethite – Gt, and hematite – Hm.

Table 1

Summary of microcosm experimental conditions, and analyses performed on each.

Set	Microcosm Type	Amendment on Day 0	Lactate on Day 10.0?	Number of microcosms, duration	Analyses
1st	Control	Amendment-free	no	Two microcosms each type, both 38.0 days	pH, Eh, dissolved elemental concentrations, As XANES, and Fe EXAFS
	Nitrate-only Treatment	Sodium nitrate	yes		
	Nitrate-Fe(II) Treatment	Sodium nitrate & ferrous sulfate	yes		
2nd	Nitrate-Fe(II) Treatment	Sodium nitrate & ferrous sulfate	yes	Two microcosms, one for 12.5 days, the other for 39.5 days	pH, Eh, dissolved elemental concentrations, dissolved organic carbon, magnetic susceptibility, magnetic separation, sequential chemical extraction/digestion, XRD, and SEM-EDS

Table 2

Steps of sequential chemical extractions. The extraction scheme mainly followed Poulton and Canfield (2005) and Keon et al. (2001). The target Fe phases were listed specifically for this study (not universally), based on sediment Fe mineralogy determined; the target As phases were listed accordingly, and were all As(V), based on sediment As speciation determined.

Step	Extractant and time	Target Fe phase	Target As phase
1	1 mol L^{-1} magnesium chloride, pH 7, 2 h, one repetition	Exchangeable Fe	Loosely bound As
2 [a]	1 mol L^{-1} hydroxylamine-hydrochloride in 25% v/v acetic acid, 48 h, one repetition	Amorphous Fe oxides (ferrihydrite)	Ferrihydrite associated As
3 [a]	50 g L^{-1} sodium dithionite, pH 4.8 with acetic acid/sodium citrate, 2 h, one repetition	Crystalline Fe oxides (goethite and hematite)	Goethite and hematite associated As
4	1 mol L^{-1} sodium phosphate, pH 5, 16 h & 24 h, one repetition for each time period	--	Magnetite adsorbed As
5 [a]	0.2 mol L^{-1} ammonium oxalate/0.17 mol L^{-1} oxalic acid, 6.5 h, one repetition	Recalcitrant Fe oxides (magnetite)	Magnetite co-precipitated As

[a] Note : the step was followed by a wash step with 1 mol L^{-1} magnesium chloride.